

K⁺ Channels and Their Modulation by 5-HT in *Drosophila* Photoreceptors: A Modelling Study

MIKA KAURANEN and MATTI WECKSTRÖM

Department of Physiology and Department of Physical Sciences, Division of Biophysics, University of Oulu, Finland

(Received 12 July 2002; accepted 25 June 2004)

Abstract—In order to clarify the role of inactivating and noninactivating K⁺ conductances in nonspiking neurons, we developed an isopotential model of the *Drosophila* photoreceptor membrane based on Hodgkin-Huxley-type equations. The model includes voltage dependent potassium conductances, the *shaker* (g_{KA}) and the delayed rectifier (g_{KS}). The model parameters were derived from published results by Hardie and coworkers and nearly identical model was used also in our previous work (J. E. Niven, M. Vähäsöyrinki, M. Kauranen, R. C. Hardie, M. Juusola, and M. Weckström. The Contribution of *shaker* K⁺ channels to the information capacity of *Drosophila* photoreceptors. *Nature*. 421:630–634, 2003). The model explains how the two types of channels function together to define the voltage dependent properties of the photoreceptor membrane. Additionally the model enables us to run simulations of conditions which are difficult to achieve in patch clamp, like prolonged membrane depolarizations by light adaptation. Effects of the activation of the delayed rectifier type conductance were found to be in accordance with published experimental work but the inactivation of the *shaker* channels, in addition to its importance in the determination of the resting potential, produced voltage amplification over equivalent passive membrane under dark adapted conditions. This phenomenon was not present in light adapted conditions. The modulation of the voltage dependence of the conductances as reported by serotonin (5-HT) caused the *shaker* to act essentially like the delayed rectifier conductance.

Keywords—Potassium channel, Simulation, Shaker, Delayed rectifier, Serotonin.

INTRODUCTION

Function of voltage dependent conductances in nonspiking cells and neurons has been studied many decades, but many aspects are still quite unclear. One model system to study these problems has been the photoreceptors of the insect compound eye, particularly those of *Calliphora vicina*. There the activation of voltage gated K⁺-channels—by a shunting and hyperpolarizing effect—oppose the depolarizations caused by the activation of the

light gated conductance. The functional role of the noninactivating, delayed rectifier type channels has been investigated extensively.^{24,27,32,41,42} In spiking neurons the inactivating K⁺-channels are able to regulate the action potential interval and frequency of spiking.^{7,8,28} Yet, although reported in several preparations^{3,4,19,30,33} other roles remain rather unclear in nonspiking cells or in graded changes of membrane potential in general. A suitable model system for studying the importance of the inactivating channels is the photoreceptor of the fruit-fly *Drosophila*. A number of papers have described several types of potassium channels in its photoreceptors cells, including a detailed characterization of slowly and fast inactivating, voltage dependent K⁺-channels.^{2,15,18,20} In particular, the *shaker* conductance is important in maintaining the signal-to-noise ratio of the graded information and it has a great importance in neural coding precision and, by virtue of its inactivation, in signal amplification.³⁵ An additional interesting feature of this system is the depolarizing shift of the voltage dependence of the potassium channels caused by serotonin (5-HT), which induces a decrease of total potassium conductance.²⁰ This feature is reportedly present also in photoreceptors of several other species.^{1,10,11} The 5-HT effects on insect photoreceptor membrane potential by actions of inactivating potassium channels has not been studied using a modeling approach before.

When enough kinetic and other data is available of membrane ionic channels, it is possible to construct models of the cell or its membrane that reproduce the electrophysiological properties of the real membrane. Membrane (or cell) model simulations may provide information of the system, when some experiments are difficult or even impossible to conduct. This applies especially to cells like insect photoreceptors, where long light adaptation times usually kill the cells when using whole-cell patch clamping techniques, when the cell interior is perfused by the pipette solution. Additionally, in *Drosophila* photoreceptors the high electrode impedances needed for good impalements usually inhibit the use of single electrode voltage clamp *in situ*, although high quality voltage recordings have been shown to be possible.^{25,26,35}

Address correspondence to Prof. Matti Weckström, Department of Physical Sciences, Division of Biophysics, P.O. Box 3000, 90014 Oulun yliopisto, Finland. Electronic mail: matti.weckstrom@oulu.fi

In this paper we derive a set of (so-called) macroscopic equations which describe the behavior of *Drosophila* photoreceptors with *shaker* and slowly inactivating delayed rectifier potassium channels under conditions where the soma voltage is the same everywhere, i.e. the cell is isopotential when the small axon is ignored. The modelling is obviously subject to inaccuracies possibly present in the experimental data which are then reproduced in the parameters derived from those. The equations have a general form familiar from the classical formulations of Hodgkin-Huxley equations²¹⁻²³ for the sodium and potassium channels in the squid axon. Here “macroscopic” means that these equations do not include biochemical state variable descriptions of the ion-channels at molecular level.^{21,23,34} Instead they are based on the kinetics defined by the opening/closing probability of the ion-channels with a defined membrane density of the channels.²¹⁻²³ The derived equations were implemented in a membrane model of the *Drosophila* photoreceptor. Our aim was to examine the general behavior of the photoreceptors with the model, including a range of membrane potentials that correspond to the light adapted state, and see what features of the behavior are caused by individual channel types, and also formulate suggestions concerning the physiological significance of serotonin modulation of the conductances, tasks that cannot, at present, be accomplished with measurements.

METHODS

Simulation Method

We developed a computer program to run simulations of the *Drosophila* photoreceptor membrane model. For the simulation we used the model development software ModelMaker (Cherwell Scientific, USA) and for some additional calculations Matlab (Mathworks, USA) was used. Equations for the channel conductances follow the normal Hodgkin-Huxley-type formalism (complete list of the specific equations which are included in the model is obtainable from the authors by request).

$$g_i = g_{i\max} \sum_k [\gamma_k(V_m, t)]^n \quad (1)$$

$$\frac{d\gamma_k}{dt} = \alpha_k(1 - \gamma_k) - \beta_k\gamma_k \quad (2)$$

$$\gamma_{k\infty}(V_m) = \frac{\alpha_k(V_m)}{\alpha_k(V_m) + \beta_k(V_m)} \quad (3)$$

$$\tau_k = \frac{1}{\alpha_k(V_m) + \beta_k(V_m)} \quad (4)$$

$$\left(\frac{g_{\infty}}{g_{\max}}\right)_k = \gamma_{k\infty}^n \quad (5)$$

$$\alpha_k = \frac{\left[\left(\frac{g_{k\infty}}{g_{\max}}\right)_k\right]^{\frac{1}{n}}}{\tau_k} \quad (6)$$

$$\beta_k = \frac{1 - \left[\left(\frac{g_{k\infty}}{g_{\max}}\right)_k\right]^{\frac{1}{n}}}{\tau_k} \quad (7)$$

g_i = conductance of channel i , V_m = membrane voltage, $\gamma(V_m, t)$ = membrane voltage and time dependent opening probability, $g_{i\max}$ = maximal conductance of channel i , E_i = reversal potential for ion i , α_k and β_k = voltage dependent kinetic variables for γ_k , n = number of k th opening probability particles, γ_4 = opening probability at steady state, $\gamma_{k\alpha}$ = contribution of the i :th steady state conductance by the opening probability particle ($g_{k\alpha}$, τ_k = time constant of the change of opening probability (γ)).

The model included the differential equations (2) needed for description of activation and inactivation of two types of conductances, the *shaker*-type and the slowly inactivating delayed rectifier K_S channels. For each time step in a model “run” the equations produced new values of α and β parameters for activation and inactivation [(6) and (7)] as a function of membrane voltage V_m [(8) and (9)]. Thereafter the *shaker* and K_S conductances were calculated using Eq. (1). The equations for the steady state contribution of the conductance by the opening probability particle (5) are of the Boltzmann type

$$\left(\frac{g_{k\infty}}{g_{\max}}\right)_k = \frac{1}{1 + e^{\frac{a-V_m}{-b}}} \quad (8)$$

and using the published²⁰ values for a and b listed in Table 1. Equations for time constants versus membrane voltage are bell shaped, and defined by²²

$$\tau_k = \frac{1}{c \cdot e^{\frac{d-V_m}{f}} + \frac{g \cdot (h-V_m)}{e^{\frac{h-V_m}{i}} - 1}} \quad (9)$$

The acquisition of parameters c , d , and $f-i$ was done by fitting the measured values (Fig. 1.) to Eq. (9) in MATLAB and the best set of parameter values for each opening probability (γ_k are listed in Table 1. The procedure of combining measured values from several sources is explained below. Equations (8) and (9) were used to achieve α_k and β_k [(6) and (7)] by using the corresponding parameter values in each case. For example following lines in the MODEL MAKER program block were written for the *shaker* activation α (amKA):

$$\begin{aligned} \text{amKA} = & (1/(1 + \exp((-23.7 - V_m)/12.8)))^0.333/ \\ & (1/(0.008174 \cdot \exp(-V_m + 1.61882)/ \\ & 24.6538) + 0.058139 \cdot (-V_m - 59.639)/ \\ & (\exp((-V_m - 59.639)/4.50122) - 1)) \end{aligned}$$

And in order to avoid zero denominator in case of $V_m = -59.693$ a conditional line was inserted as follows:

$$\text{if abs}(\exp((-V_m - 59.639)/4.50122) - 1) < 1e - 7$$

$$\text{amKA} = (1/(1 + \exp((-23.7 - V_m)/12.8)))^0.333/$$

TABLE 1. Numerical values for Eqs. (6)–(9).

	KA activation	KA inactivation	KS activation	KS inactivation
a (mV)	-23.7	-55.3 2nd -74.8	- 1	-25.7
b (mV)	12.8	-3.9 2nd -10.7	9.1	-6.4
c (ms ⁻¹)	0.0082	0.2303	0.11626	—
d (mV)	1.619	-192.97	-25.655	—
f (mV)	24.654	31.32	32.19	—
g (ms ⁻¹ mV ⁻¹)	0.05814	0.04373	0.0066	—
h (mV)	-59.64	13.486	-23.803	—
i (mV)	4.50	11.11	1.345	—

Note. The weight of the 1st inact. comp. is 0.8 and the 2nd is 0.2.

$$\frac{1}{(0.008174 * \exp((-V_m + 1.61882)/24.6538) + 0.058139 * 4.50122 * (1 + (V_m + 59.639)/(2 * 4.50122)))}$$

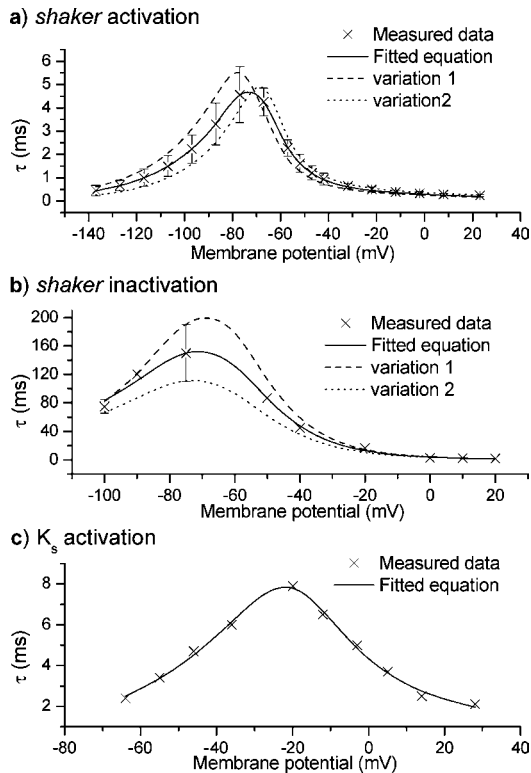


FIGURE 1. (a) Time constant of activation of *Drosophila* photoreceptor *shaker* (g_{KA}) channels in function of membrane voltage. Experimental values are marked by + and the line shows the fitted equation. Also two variations are plotted as extreme cases defined by error bars. (b) Time constant of inactivation of *Drosophila* photoreceptor *shaker* (g_{KA}) channel versus membrane voltage. The crosses show the experimental values and the line the fitted equation. Two variations are also plotted. (c) Time constant of activation of *Drosophila* photoreceptor slow delayed rectifier channel (g_{KS}) versus membrane voltage. The crosses show the experimental values and the line the fitted equation.

A flow diagram of the simulation program and a schematic figure of the membrane with its ion channels is described in Fig. 2. The folded membrane is the microvillar part of the cell which effectively increases the capacitance of the cell.

In the current clamp simulations (that is, when no “voltage clamp” was used) the membrane voltage was obtained using the typical differential equation

$$\frac{dV_m}{dt} = \frac{I_m}{C_m} - [g_{KS}(V_m - E_K) + g_{KA}(V_m - E_K) + g_l(V_m - E_l) + g_{LIC}(V_m - E_{LIC})]/C_m \quad (10)$$

in which C_m is the membrane capacitance per membrane area and g_{KS} , g_{KA} , g_{LIC} , and g_l are (per membrane area), respectively, the conductances of the fast delayed rectifier, the *shaker*, (1) the light dependent conductance, and the leak conductance independent of voltage and light, and E_K , E_{LIC} , and E_l are the equilibrium potentials of potassium, light dependent conductance, and the leak, respectively. Conductances g_{KS} and g_{KA} are time and voltage dependent. In the model I_m is expressed as (clamped) current density.

Acquisition of Parameter Values for the Model

Shaker Channel g_{KA}

Data for the *shaker* channels' steady state opening probabilities and time constants for activation and inactivation were obtained from published studies.^{2,15,18,20,35} The steady state inactivation (8) is sum of two components.²⁰

It is evident from the recordings of *shaker* currents in the cited papers that the activation does have more than one gating particle. In our macroscopic model we set n to be three.³⁸ According to Hevers & Hardie²⁰ authors report that they had better and more stable conditions in patch clamp measurements than published previously.¹⁵ Thus, they derived activation function of the voltage dependent conductances that were shifted +23 mV compared to earlier findings. In accordance to this similar values were also published.² Knowing this we shifted voltage axes by

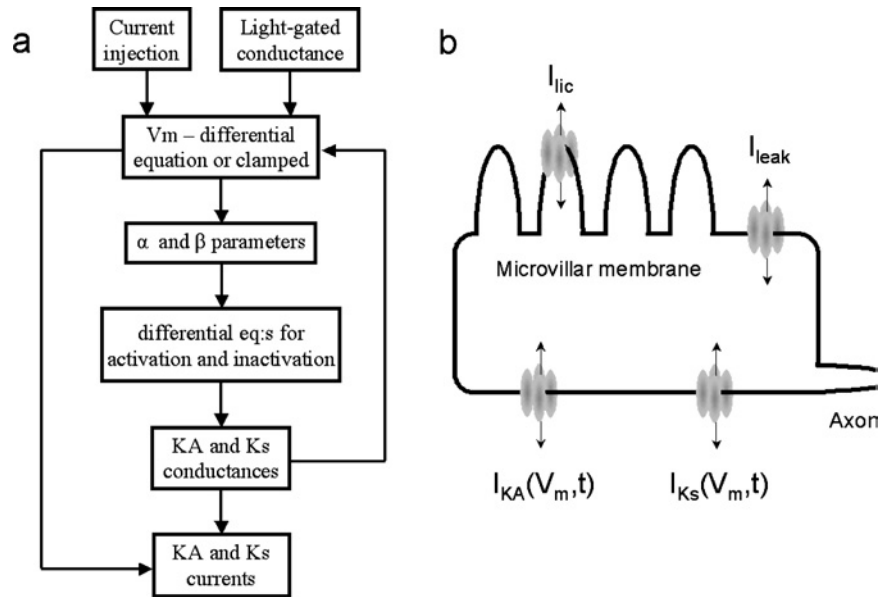


FIGURE 2. Scheme of the model we used. (a) Description of the modelling program. The calculated values may be obtained at any stage in the process. The arrows show the direction of data flow between each time step. (b) A schematic figure of the photoreceptor, with its (in this model) isopotential soma, microvillar membrane with the light gated current (I_{LIC}), and the nonmicrovillar membrane with the three currents, the *shaker* (I_{KA}), the delayed rectifier (I_{KS}), and the leak current (I_{leak})

+23 mV when analyzing the time constant values obtained from Hardie.¹⁵ Thus in time constants of *shaker* activation have, as a function of membrane voltage, a typical bell-shaped function as shown in Fig. 1(a). The error bars show the variation limits of the time constant and two “extreme” cases (variation 1 and 2) have been plotted for testing of the sensitivity of the model behavior to time constant variation.

Time constants of *shaker* inactivation as a function of membrane voltage were obtained from published data.^{15,18,35} A similar kind of voltage shift as previously mentioned was found²⁰ as compared to reference¹⁵ in the parameter values of *shaker* steady-state inactivation. Here the shift was +13.7 mV. In accordance with our supposition that the newer set of data is superior to the old ones, we shifted the voltage axis by +13.7 mV in analyzing the time constant of *shaker* inactivation¹⁵ (measured data from -100 mV to -90 mV) and¹⁸ (this data used in combination with data from reference³⁵ at data points from -50 mV to +20 mV). The resulting bell-shaped function for the *shaker* inactivation is shown in Fig. 1(b). Variations 1 and 2 are also plotted to be used in testing purposes.

Slowly Inactivating Delayed Rectifier Potassium Channel g_{KS}

Data for the steady state opening probabilities and time constants for activation and inactivation of the *Drosophila* slowly inactivating channel were collected from published data.^{2,15,20}

Values of τ for KS activation were obtained from Hardie.¹⁵ Again, the voltage axis was shifted, in this case by

+11 mV.²⁰ Resulting plot of time constants of the delayed rectifier activation as a function of membrane voltage is shown in Fig. 1(c). Here no variation data were available.¹⁵ The g_{KS} activation is best fitted by two particle gating,¹⁵ and the n in Eqs. (6) and (7) is thus 2. This was also reported in association with time constants by Hardie.¹⁵

The τ of g_{KS} inactivation was reported to be between 1000 to 3000 ms¹⁵ but no accurate information of its voltage dependency has been shown. We used a constant value of 1400 ms in our equations.

Conductances and Leak Reversal Potentials

Maximum values for the various conductances and the value for the membrane capacitance were calculated on the basis of data in the published reports of *Drosophila* photoreceptor potassium channels where patch clamping data from isolated photoreceptors R 1–6 (short visual fibre) were used.^{15,20} The calculated photoreceptor membrane area was about $1.2 \cdot 10^{-5}$ cm², the maximal value for the *shaker* conductance density was 5 mS/cm² (1) and the same was found to be acceptable for the delayed rectifier. Only R1–R6 type photoreceptors were of concern here, because they have been suggested to deal with contrast coding,³¹ and also form a functionally homogenous group in the retina.¹⁴ The amount of the fast inactivating delayed rectifier, K_F , has been reported² to vary a lot in these cells and they seem to have much smaller significance than *shaker* and KS channels. Thus one simplification we did was that this type of conductance was not included in the model. The total nonvoltage dependent conductance in the model is a

sum of two conductances, g_{LIC} and g_1 . The first, the g_{LIC} , represents the light gated conductance and g_1 is the light independent conductance. The g_{LIC} was used nondynamically in order to polarize the membrane to a desired (simulated) light adapted voltage level, but also in attempts to simulate effects of voltage dependent conductances on voltage responses to a brief light pulse. Assuming a “mixed” cationic conductance as described by several investigators,^{16,17,37} the reversal potential of g_{LIC} was set to 0 mV.

When the value of the g_{LIC} was set to zero, the choice of the light independent leak conductance, the g_1 , was constrained so that the V_m (the membrane voltage) reached the value of -65 mV and the model produced an input resistance 170 M Ω for the model cell. To obtain this, the reversal potential of the g_1 was set to -55 mV, representing an unspecific leak conductance responsible for the fact that resting membrane voltage is considerably above the equilibrium potential of potassium (-85 mV), and conductance was set to 0.314 mS/cm². The actual observed dark resting membrane potential -60 mV was obtained by an insertion of a very small value of the g_{LIC} conductance (0.053 mS/cm²). The light independent leak component could not be omitted from the model because it was found to be necessary for the membrane potential stability. Without the leak conductance the *shaker* conductance’s strong voltage dependent inactivation and a large window current around -50 mV tended to force the V_m to be bistable, and to go either near -60 mV or to near -30 mV, depending on the instantaneous value of the speed of the change of the V_m during the particular simulation. The obvious reason for the bistability is the positive feedback produced by *shaker* inactivation (see below in this paper). It has to be observed that the equilibrium potential of the leak conductance had to be more positive than the normal resting potential in order to counteract conductance of both the delayed rectifier and the *shaker* window current. This is in accordance with the basal values of the noninactivating conductance in the blowfly photoreceptors, where the activation of the delayed rectifier conductance is playing a similar role as the *shaker* apparently does in *Drosophila*.⁴¹

Capacitance

Membrane capacitance estimation in microvillar photoreceptors is somewhat complicated, and cannot be done only on the basis of the membrane area, because the microvillus forms a large part of the membrane that is not contributing equally to the resistive (i.e. to the leak and to the voltage dependent conductance) and capacitive part of the cell.^{32,41} The measured values of the total cell capacitance for adult *Drosophila* photoreceptors are in the range of 30 pF¹⁵ and 52 pF.² The calculation of the microvillar area gave us an estimate of 48 pF, which is close to those in the latter estimates. Thus, if we use the nonmicrovillar membrane area as the estimate for the resistive

membrane, the membrane capacitance value of a patch of membrane as a representation of the whole cell had to be set to 4.0 μ F/cm², significantly higher than the normally used 1 μ F/cm², to take into account the extra microvillar membrane area. This causes the photoreceptor cells to be more low passing than would otherwise be expected (for further considerations along these lines, see,^{32,42} for discussion).

A further fundamental assumption in the modelling was that the changing ionic conductances, and the consequent ionic currents did not change the equilibrium potentials of the ions even in light adaptation (as supported by experiments in *Calliphora* photoreceptors⁴¹). Also all other possible modulations other than by 5-HT were ignored in the modelling, including a possibility that the exceptionally elevated intracellular calcium in light modify some of the properties of the voltage dependent or leak channels.³⁶

Effect of Individual Channel Types

When simulations were run using membrane models containing both the delayed rectifier and *shaker* conductances, or either one of these alone, the total potassium conductance (i.e. sum of g_{KA} and g_{KS}) at the same steady state membrane potential was set to be equal in each case to facilitate comparison of different membrane designs with different channel composition. That was achieved by increasing the maximal conductance (1) for the channel type that is alone on the membrane. With the same membrane resting potential the leak conductance g_{LIC} was unaltered throughout.

Simulation Procedures

The protocols in current clamp simulations [representing I_m in Eq. (10)] were produced by the model program. Voltage changes were then generated using the Eq. (10). In voltage clamp simulations the differential equation for V_m (10) was excluded and replaced by a program which forced the desired voltage values. Simulated potassium currents (I_{KS} and I_{KA}) were produced as dictated by the HH-type equations and with $I = g_K(V_m - E_K)$ where g_K is the corresponding K⁺ conductance.

In simulations of the light responses we used a purely phenomenological form of the light gated conductance, which is not supposed to have any causal connection to the transduction. The g_{LIC} was altered (10) to produce a smooth pulse of light current with an “adaptation” having a time course similar to real currents. Equation (11) represents the light induced activation (10 ms from the beginning of the model run)

$$g_{LIC} = g_{LIC}(0) + (0.0015 - g_{LIC}(0)) \left(1 - e^{-\frac{t-10}{5}}\right) \cdot e^{-\frac{t-10}{200}} \quad (11)$$

and Eq. (12) the relaxation (after t_{lightoff})

$$g_{LIC} = g_{LIC}(0) + (0.0015 - g_{LIC}(0))$$

$$\left(1 - e^{-\frac{t-10}{5}}\right) \cdot e^{-\frac{t-10}{200}} \cdot e^{-\frac{t-\text{highoff}}{5}} \quad (12)$$

Changes in V_m , I_{KS} , and I_{KA} were then calculated, using the current clamp mode of the simulation. The maximum value for the light gated conductance was the same in all simulated cases, again to facilitate comparisons between different cell membrane models. Although the light responses are not meant to simulate the real light responses, they resemble the real sequence of events producing the light gated current in real photoreceptor cells in the sense that the membrane voltage is changed by increasing a depolarizing conductance. Thus for the present purposes these simulations are realistic enough, and help in displaying the dynamic behaviour of the model cell when the membrane conductance is changing, as in real photoreceptors.

Production of the 5-HT Modulation

Effect of serotonin (5-HT) modulation on *Drosophila* photoreceptor potassium channels has been reported in detail.²⁰ This included a positive shift in the voltage operating range, of as much as 30 mV for the *shaker* channels and up to 14 mV for the slowly inactivating delayed rectifier channels. In the present work these shifts were included in the equations determining the conductances g_{KS} and g_{KA} [in Eq. (10) and in parameters a , d , and h in Eqs. (8) and (9)]. In the 5-HT modulated membrane model the maximum of both voltage dependent K⁺ conductances (g_{KS} and g_{KA}) was set to 5 mS/cm² which is equal to the normal (unmodulated) case. When one of the conductances was omitted, the maximum K⁺ conductance was increased to obtain the same resting or light adapted voltage level. Light conductance values required in order to achieve the desired membrane holding potential and thereby to produce light adapted membrane voltage were necessarily different from the nonmodulated case. This is because the steady state conductances were altered by the shifts of the voltage operating ranges of the channels, especially by the change of the *shaker* window current.

TESTING EQUATIONS BY SIMULATION

To ensure that the simulation, where the model parameters were derived from the voltage- and time-dependence of the currents, reproduces similar currents as observed experimentally we first tested the *shaker* and KS activation and inactivation at varied membrane voltages by small voltage steps and verified that the simulated currents matched the experimental ones (the data is not shown for their simplicity and multiplicity). An exemplary comparison to quite complex experiments is shown in Fig. 3. Here the membrane voltage was stepped to +10 mV after a range of hyperpolarizing prepulses of -20 to -110 mV. In all sets [both simulated (b) and experimental (a)] the *shaker* current (I_A) is almost completely inactivated with prepulses to mem-

brane voltages to -50 mV or above. The shapes of the simulated membrane current densities [Fig. 3(b)] are close to the experimentally found ones [Fig. 3(a)].

In this type of comparison an exact match of the simulated currents with any experimental current cannot be expected, because in the original experiments the magnitudes of the currents varied significantly from cell to cell, much more than the differences here between simulations and experiments. Thus the model parameters were derived on the basis of the averaged properties. In this simulation the *shaker* maximal conductance was twice than in other simulations (i. e. 10 mS/cm² vs. 5 mS/cm²). In subsequent simulations the individual and combined effects of the channel types were the main point, not to get exact match with experimental results.

The variation in the experimental data allowed us to determine corresponding variations of the *shaker* time constants, which effects are shown for the prepulse -110 mV [Fig. 3(c)]. Here the first number refers to activation variation and the second to inactivation variation [Fig. 1(a,b)]. The transient peak-current is reduced with higher *shaker* activation time constant (variations 22 and 21) and the transient lasts a bit longer with higher *shaker* inactivation time constant (variations 11 and 21). No other significant effects are seen by variations of *shaker* time constants. More effect has the proportional amount of *shaker* and KS conductance [Fig. 3(d)]. This is quite evident, though, that with higher *shaker* conductance the transient current peak is higher and vice versa. Variations in proportional amounts of *shaker* and KS conductances just cause the responses to show more of those effects that are connected to the individual channel behavior as also shown later (Fig. 6). With this in mind we judge that the responses in Fig. 3 correspond to those reported in the original papers, and we consider the simulation successful in this sense.

RESULTS OF SIMULATIONS

Voltage Clamp Simulations of the Model

Voltage clamp simulations (Fig. 4) were run to see the time courses of the activated conductances both in the case of dark (DA) and light adapted (LA) membrane, and also when the voltage-dependences of the conductances were shifted into more depolarized voltages, as reported by the serotonin (5-HT). For voltage and also for current clamp simulations the resting membrane voltage of the model in DA and LA was set by changing g_{LIC} (as explained in Methods). The net membrane current was zero at the resting potential, but in the resting state the current in Fig. 4 is always slightly positive because only the potassium current is shown. The figures show (in addition to the voltage protocol used, topmost trace) the membrane potassium current densities (middle) and the values of the KS and *shaker* conductances (below, only the traces corresponding to the

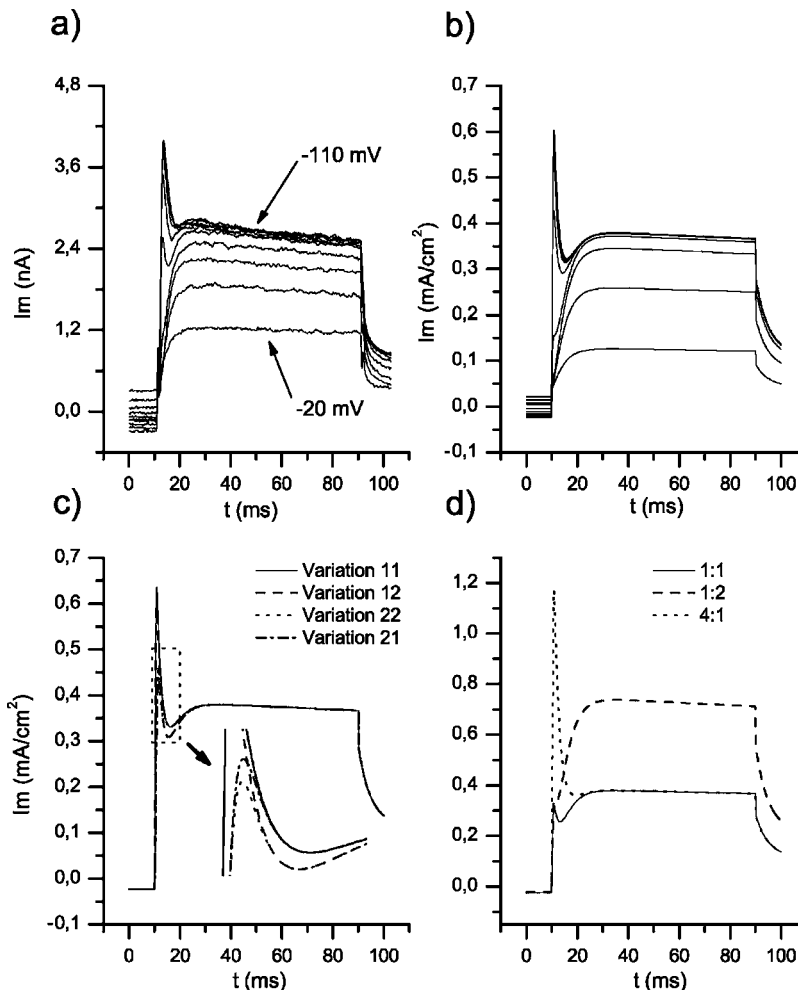


FIGURE 3. Comparison of experimental potassium current data of *Drosophila* photoreceptor³⁵ (a) and simulated *Drosophila* photoreceptor potassium current densities (b). The membrane was stepped to +10 mV after varying prepulses from -110 mV to -20 mV. Note the amount of total currents and the ratio of I_{KS}/I_{KA} vary much from cell to cell. Effects of variation as of *shaker* time constants. The inset shows the differences in smaller scale (c). Effects of variations of individual channel type conductances (d).

smallest and the largest voltage step are shown). With dark adapted membrane [Fig. 4(a)] a fast transient at the beginning of voltage steps was caused by the activation of the fast *shaker* current (dotted line). As expected, the time constants of inactivation of this transient were reduced with increasing depolarization. With more depolarized steps progressively more delayed rectifier current was also activated (continuous line). With 5-HT-modulation [Fig. 4(b)], i.e. a depolarizing shift of the activation and inactivation functions, the currents were formed by a clear combination of both currents, the main difference created by the slower inactivation of the *shaker*, making its contribution larger.

Current Clamp Simulations

In the current clamp simulation the V_m (10) was calculated with depolarizing current injections that were increased by 4-mA/cm² steps and had a duration of 200 ms.

Responses were [Fig. 5(a)] like those of a passive RC-circuit during the first 10 ms, but were then followed by a sudden decrease in the expected slope of the voltage, caused by the *shaker* activation (the lower trace, dashed line). Thereafter the voltage began to rise again, because of the subsequent *shaker* inactivation. The *shaker* conductance was then decreased by inactivation to values well below those at the resting state. The *shaker* inactivation thus acted as a depolarizing booster. The more depolarized was the voltage, the bigger was the shunting effect caused by the increasing activation of the delayed rectifier conductance, responsible for the plateau of the responses to the two largest current steps. Consequently, the V_m did not increase as much as expected with increasing current pulses. With first three pulses the shape of the voltage response was dominated by action of the *shaker* conductance, whereas the effect of the delayed rectifier increased with more depolarizing pulses. The obvious reason is that the half activation and inactivation

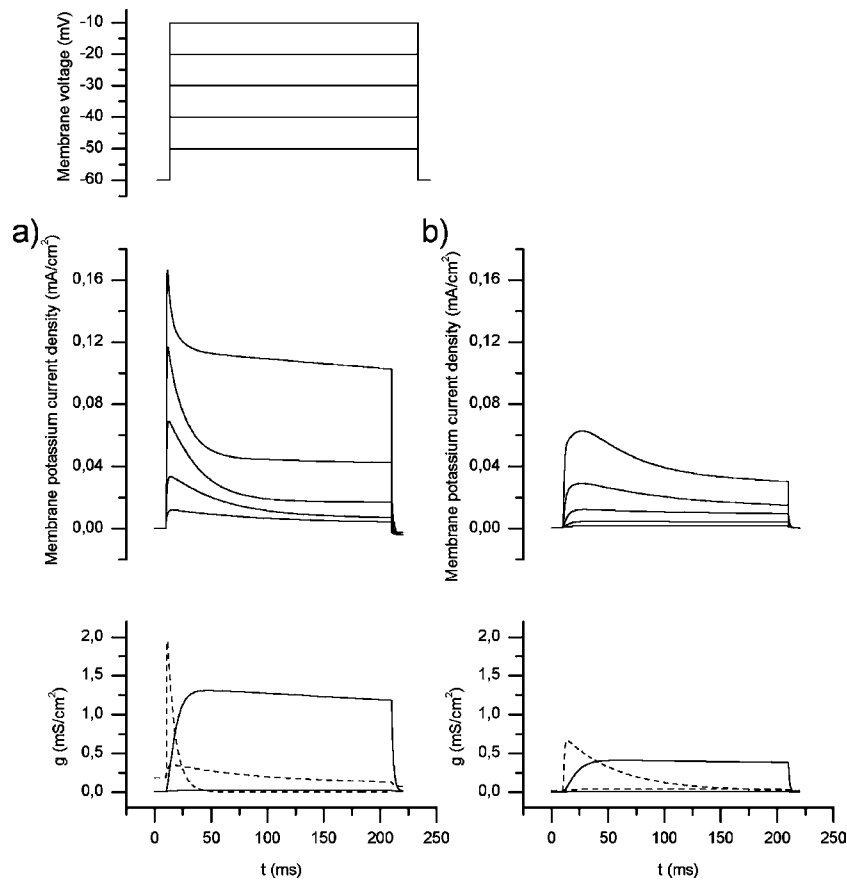


FIGURE 4. Simulated voltage clamp currents of the *Drosophila* photoreceptor membrane model in dark, holding potential -60 mV, and command steps as shown in the uppermost traces. (a) Without 5-HT; the upper traces show the voltage clamp currents, and the bottom traces show the corresponding conductances (g_{KA} dashed; g_{KS} continuous) with the smallest and largest voltage command step. (b) With 5-HT. The traces as in (a).

voltages of *shaker* were -23.7 mV and -55.3 mV, and that for the delayed rectifier these are much more depolarized, -1.0 mV and -25.7 mV, correspondingly.²⁰ Responses of the light adapted (but nonmodulated) membrane [Fig. 5(b)] showed clear depolarizing notches at the beginning. Here the delayed rectifier was the dominating voltage dependent conductance, and the *shaker* contribution was almost nonexistent.

The DA membrane with 5-HT showed voltage responses to current pulses that were close to those of a passive membrane, i.e. of a RC circuit [Fig. 5(c)]. This was to be expected because the effect of 5-HT was to shift the activation and inactivation ranges of both conductances to more positive values, and the activated amount of both conductances is small. The contribution of the *shaker* conductance was more prominent. With modulation the voltage responses of the LA membrane [Fig. 5(d)] show typical effects of an inactivating outward current. Shifts of the potassium channel characteristics induced by 5-HT make *shaker* activation and inactivation prominent again, also at voltages around $+30$ mV. Differences in responses [in Fig. 5(d) compared to Fig. 5(a)] are mainly caused by the increase of

the conductance producing the light-adaptation (g_{LIC}) and the lower *shaker* inactivation. Depolarizing notches at the beginning in Fig. 5(d) are caused by relatively slow activation of *shaker* current. In experimental recordings like Fig. 5(d) the investigator (without any prior knowledge of the conductances) is likely to erroneously interpret the slow depolarization in response to a current pulse as reflecting the membrane charging characteristics (i.e. passive membrane), whereas it is caused by slow changes in voltage activated conductances.

Light Response Simulations

We produced a rough simulation of the conductance change for steplike light input with the model (see Methods). Membrane voltage responses to this simulated input are depicted in Fig. 6 (insert above shows the time course of the g_{LIC}). The simulations here were done to examine the responses of four different membrane designs: the passive case (no voltage activated conductances, traces marked "passive"), the cell with either of the voltage activated conductances present (traces marked " g_{KS} "

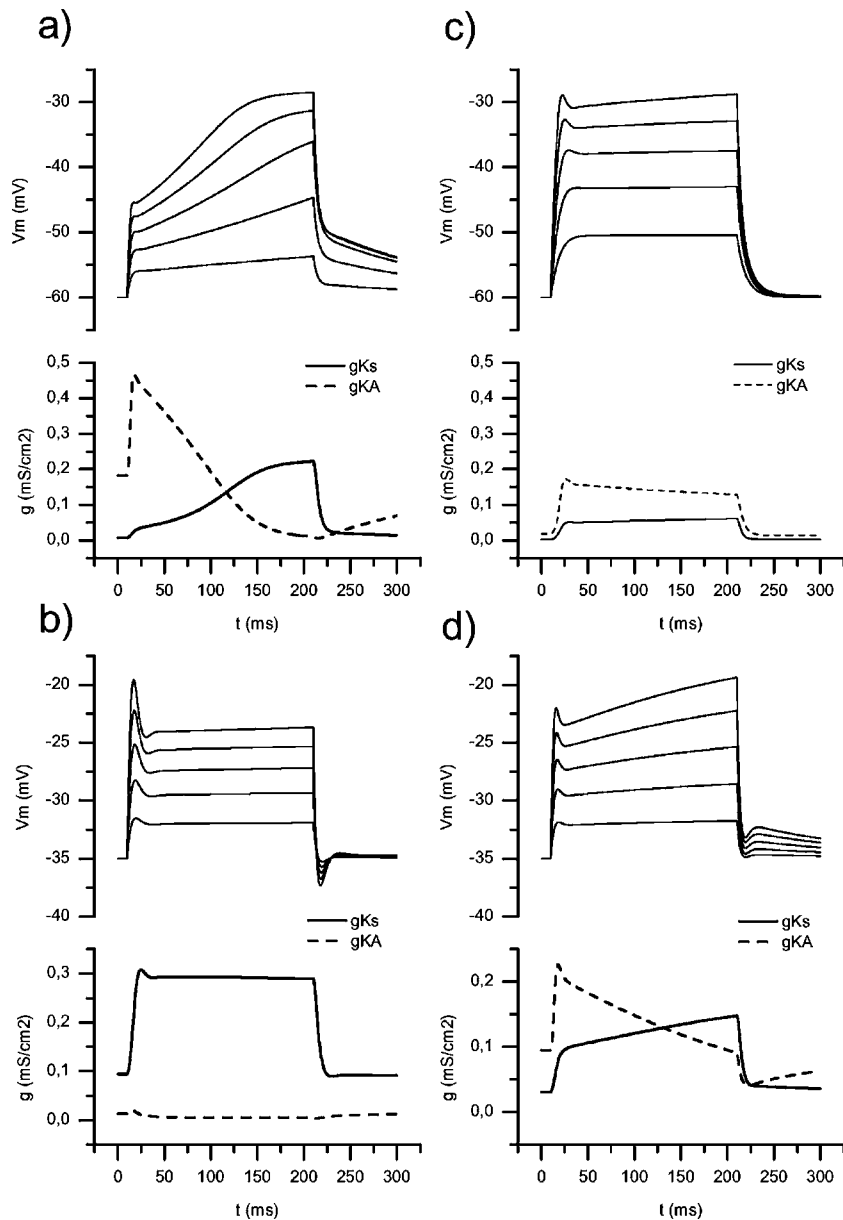


FIGURE 5. Simulated current clamp experiments of the *Drosophila* photoreceptor membrane model. The cell was stimulated with five 200-ms current steps that were increased by 0.04-mA/cm^2 intervals. In each figure, the upper traces show the membrane voltage in response to the current injection, and the lower traces show the corresponding conductance changes (g_{KA} dashed; g_{KS} continuous) for the largest current step of 0.2 mA/cm^2 . (a) Dark adapted without 5-HT. (b) Light adapted without 5-HT. (c) Dark adapted with 5-HT. (d) Light adapted with 5-HT.

and “ g_{KA} ,” with the conductances matched as explained in the Methods), and the case where—as in all the preceding simulations—both conductances were present (traces marked “Both”).

The dark adapted (resting potential at -60 mV) set of responses for the normal, nonmodulated case is shown in Fig. 6(a), with the voltage responses in the upper, and the activated conductances in the “both” case shown in the lower set of traces. The membrane with *shaker* alone produced bigger voltage responses than the passive membrane,

supporting the findings in Fig. 5(a), where *shaker* inactivation acts as a relative amplifier of the responses. When the membrane only had the delayed rectifier, the response was smaller than in any other case, and a voltage peak was seen at the beginning. The response of the membrane containing both types of conductances was clearly a combination of the responses. Here the *shaker* was activating and inactivating fast, and the delayed rectifier had relatively slow activation because of the slow development of the depolarization caused by rapid activation of the *shaker* conductance.

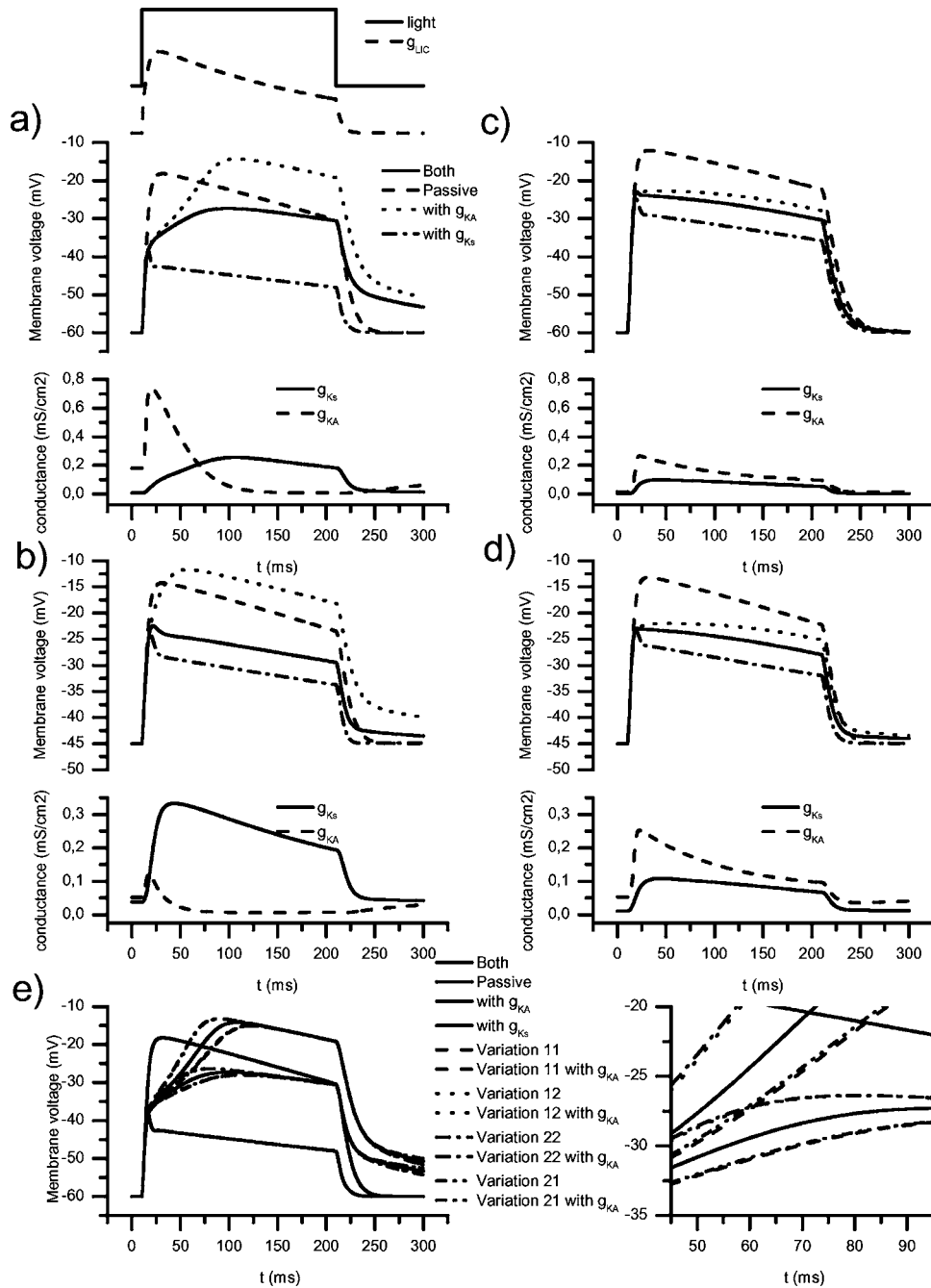


FIGURE 6. Simulated light responses at different adaptation levels and comparison of membranes with and without the voltage dependent conductances. The total potassium conductance at steady state is the same in each case. The timing of the light stimulus and the time course of the activated light gated conductance (g_{LIC}) is shown inserted in the upper left corner. The figures show [as indicated by the key by (a)] in the upper traces the voltage responses to light, and in the lower traces the corresponding conductances (g_{KA} dashed; g_{KS} continuous) in the case where both the voltage dependent conductances are present. (a) DA, (b) LA, (c) DA with 5-HT modulation effect, (d) LA with 5-HT modulation effect, (e) Effect of *shaker* time constant variations on experiment (a) (left) and the most important parts with smaller scale (right).

Simulation of the light adapted situation is shown in Fig. 6(b). Again when the membrane only had the *shaker*, the voltage response is bigger than with the passive membrane. Smallest response is generated with only the delayed rectifier present. Voltage response of the membrane

with both conductances is qualitatively near the response of the membrane with the delayed rectifier alone, because the *shaker* channels were largely inactivated with the depolarized membrane potential and their contribution is small [compare Fig. 5(b)].

The results from the simulation of the dark adapted 5-HT modulated case are shown in Fig. 6(c). Voltage response with *shaker* alone did not exceed the response of the passive membrane as was the case in Fig. 6(a) and 6(b). With both conductances present the response was similar to the responses with *shaker* alone. This is because the amount of the delayed rectifier conductance was small compared to *shaker* conductance at voltages produced, and because the *shaker* acts now kinetically more like the delayed rectifier (as seen in the lower traces). Voltage response of the membrane with delayed rectifier alone was qualitatively similar as Fig. 6(a) and 6(b), but the hyperpolarizing effects were smaller because of smaller activation of the conductance.

LA membrane in 5-HT modulated situation [Fig. 6(d)] show responses that were much like those in dark adapted and modulated case [Fig. 6(c)], but the amount of the delayed rectifier conductance was now increased. Here the *shaker* behaved more like the delayed rectifier conductance, albeit with faster inactivation. This was also the major difference to light adapted nonmodulated case [Fig. 6(b)].

Results from *shaker* time constant variations [Fig. 1(a) and (b)] are shown in Fig. 6(e). Here the Fig. 6(a) is replotted with simulations with variable time constants. With the multitude of different lines a zoom in from the most important part of the plot is shown at right. Here the importance of *shaker* inactivation can clearly be seen. The faster the inactivation (variations 12 and 22), the bigger is the amplification caused by it.

In experiments the light responses of photoreceptor cells are often tested with short flashes of light. The effects of the conductances and 5-HT on those are shown in Fig. 7 in dark adapted conditions. Using a simulation for a response to a flash of 10-ms duration the activation of the light gated conductance g_{LIC} (in upper left) caused a response of about 25 mV. Here the delayed rectifier was activated to a very small extent, but the g_{KA} activated rapidly during depolarizations [Fig. 7(a)]. The g_{KA} then inactivated, again beyond the resting value. This coincided in the response with the repolarization phase. Thus the inactivation of *shaker* tends to prolong short responses by the depolarizing effect of the decreased K^+ -conductance. In the 5-HT modulated case [Fig. 7(b)] both conductances were activated only to a small extent, and, consequently, the voltage response was significantly bigger (about 35 mV), and the repolarization was significantly faster, lacking the depolarized “tail” in the response in Fig. 7(a).

DISCUSSION

The main impact of the present work is in clarifying—beyond what can be done by experimentation—the role of the two main conductances, the *shaker* and the KS, in *Drosophila* photoreceptors, and the proposed serotonin modulation thereof.²⁰ In nonspiking neurons the function of the inactivating potassium conductance is not

as well understood as it is in the spiking neurons, although they have been described in several types of photoreceptors and neurons, both in invertebrates and in vertebrates.^{3–6, 15, 19, 29, 30, 33, 39, 40, 44}

Equation Determination and Sensitivity Analysis

As an attempt to explain in detail the function of fast inactivating K^+ channels we have successfully constructed a set of macroscopic models for the *Drosophila* photoreceptor membrane that contain conductances such as those formed by the voltage dependent potassium channels, of the fast inactivating *shaker* and slow inactivating KS channel types. The models were based on recordings^{2, 15, 20, 35} which were not originally designed in order to model the cells with Hodgkin-Huxley type equations.^{21–23} Some of the differences between the output of our model and the published experimental data may be due to the natural variation of many of the modelled parameters, but we believe to have obtained the useful values for describing the kinetics of the ionic conductances. Variation in the parameters would shift the operating voltage ranges of the actions we found with the model. Changes in the parameters would not totally exclude these effects but would alter their magnitude (see later). Construction of state transition based models^{21, 23, 36} (like that developed for *Drosophila* muscle *shaker* channel⁴⁵) were not needed, because we were interested only in the macroscopic conductance produced by the channels. Also any changes in the ionic concentrations, that should be considered if the modelling were based on the GHK-equations^{12, 13, 23} was not included in the model. The models we used describe the membrane of an isopotential cell. Although this is clearly a limitation, the insect photoreceptors with short axons are apparently isopotential when the somata are considered.^{15, 41, 42} The use of the isopotential model also reduces errors caused by estimation of the possible spatial spread of current. Thus the present modelling exercise can be justified as a means to obtain information of the membrane behavior under conditions which cannot be maintained in experiments, such as prolonged, depolarizing light adaptation.

In a model of the *Drosophila* muscle *shaker* channels four closed states have been assumed.⁴⁵ However, the muscle *shaker* channel is molecularly different from the *shaker* found in *Drosophila* neurons. In addition, in other published Hodgkin-Huxley type^{21–23} models for the fast, inactivating potassium current we can find values of the exponent ranging from 1 to 4, the majority using the value three.³⁸ Therefore, the exponent in Eq. (1) related to the number of assumed closed states of *shaker* was chosen to be 3.

The biggest potential source of error in our model construction is the voltage dependence of the time constants for *shaker* activation and inactivation, and those for KS activation as they can alter the operating voltage ranges of the effects we found. This is mainly caused by somewhat

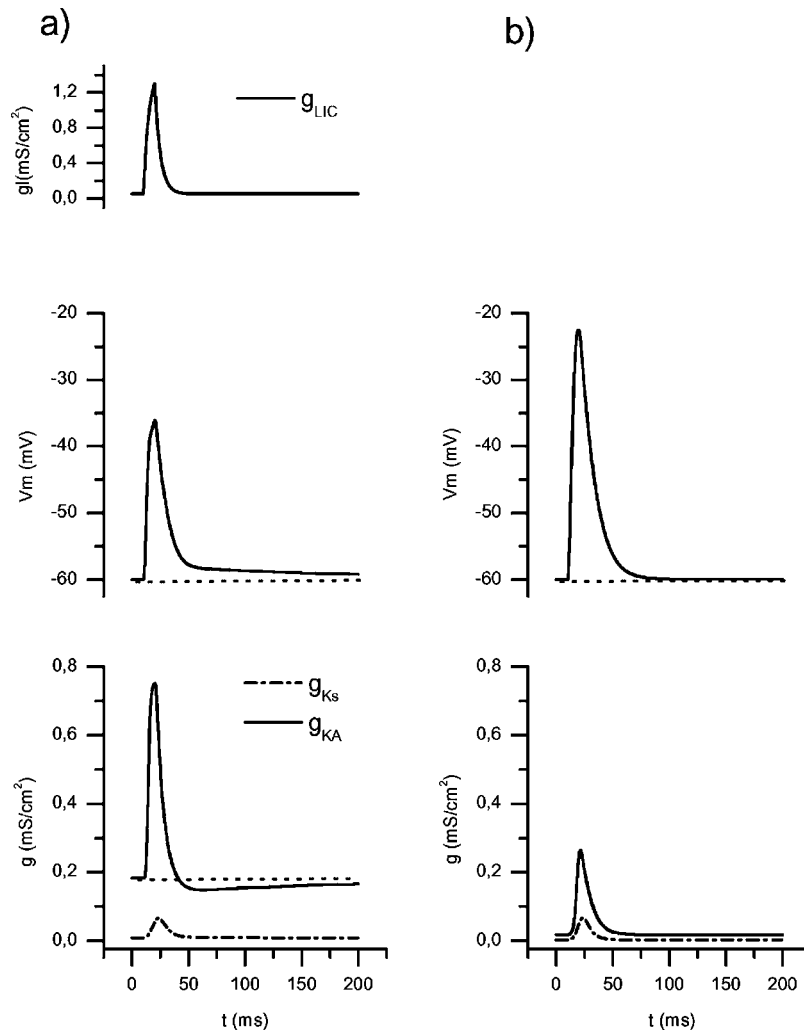


FIGURE 7. Simulation of responses to short light flashes of 10-ms duration. (a) upper trace shows the activated conductance by light, middle trace is the generated voltage response, and the lower trace shows the time courses of the voltage activated conductances (g_{KA} continuous; g_{KS} dashed). (b) the voltage response (upper) and voltage activated conductances (lower curve) with 5-HT modulation. Conductances as in (a).

conflicting results in the original papers from where the data were retrieved. Given that the insect photoreceptors are functionally very fragile in whole-cell patch clamping experiments—which is one main justification for this modeling work—we assumed that the newer set of data^{2,20,35} is the most accurate one. However, not all of the parameters could be obtained from there, and the older set of data^{15,18} had to be used with suitable adjustments to fit the newer findings.

Simulated responses [Fig. 3(c) and Fig. 6(e)] with the variations of *shaker* time constants [Fig. 1(a) and Fig. 1(b)] do not show very impressive effects on the responses. Results in Fig. 3(c) and in Fig. 6(e) can thus be considered as sensitivity analysis for *shaker* time constant variation within experimental limits. As Fig. 6(a) with only *shaker* conductance on the membrane is one of the most important results of this work, further sensitivity analysis was performed for the parameters maximal *shaker* conductance

($g_{KA_{Am}}$), nonspecific leak conductance (g_l), its reversal potential (E_l), and light activated leak conductance reversal potential (E_{LIC}) in this simulation (Fig. 8). These variations of parameters around their determined values do not show any qualitatively significant effects on the results. Variations of E_{LIC} [Fig. 8(d)] cause only more or less driving force for the light activated input in these simulations. The effects of shifts in the voltage operating ranges in *shaker* steady state conductances (5) have more remarkable effects. This is discussed below.

Determination of Parameter Values

Maximal conductance values in Eq. (10) were derived from the published measurements of *Drosophila* photoreceptor potassium currents,^{15,20} based on the maximal current, and assuming that the maximal currents are equal to the saturated ones. There are some concerns related to these.

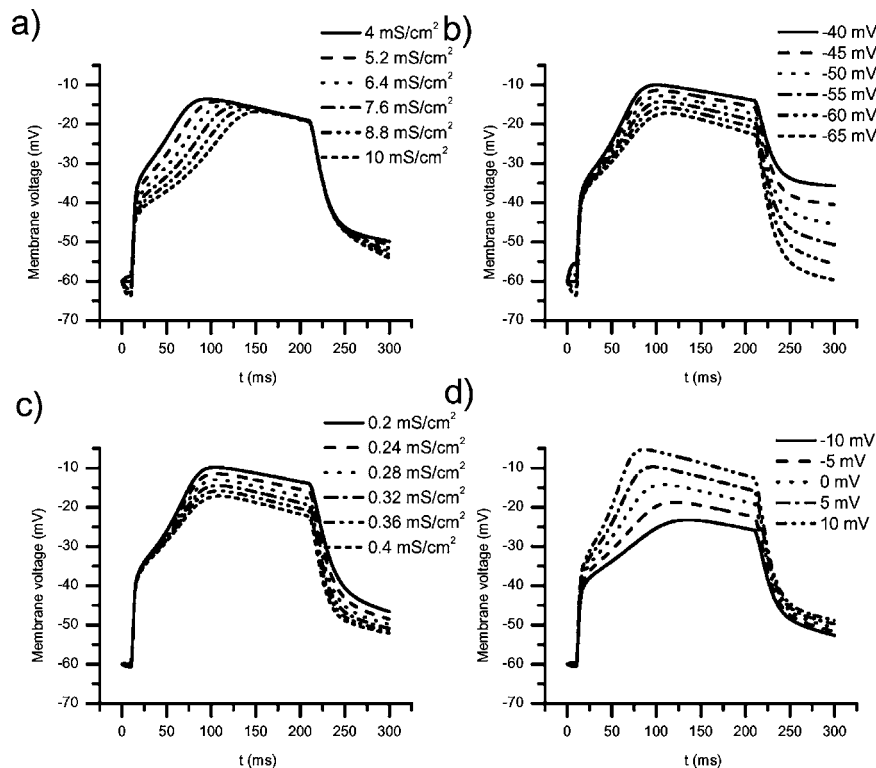


FIGURE 8. Sensitivity analysis on the experiment in Fig. 6(a) with *shaker* conductance only by variations of parameters: (a) maximal *shaker* conductance, (b) nonspecific leak reversal potential, (c) nonspecific leak conductance, (d) light activated leak reversal potential.

A small but uncontrolled amount of inactivation might be present in the measurements. In addition, there is a possibility of contribution from other currents, or that the currents recorded might simply not have reached saturation. Yet, given these caveats, and as the effects of variations of the proportional amounts of individual conductances were also simulated [Fig. 3(d)], the modelling reproduced the membrane behavior closely (see Fig. 3). Individual contributions of *shaker* or delayed rectifier conductances on the responses of the membrane were also tested in conjunction with the simulated light responses (Fig. 6), which enabled us to estimate how the responses of the membrane would change if the ratio of the maximal conductances of the *shaker* and KS were different from those used in the present modelling.

Properties of the Shaker Conductance

The activation and inactivation of the *shaker* current is in the so-called “window current” area near -50 mV in the nonmodulated case [Fig. 9(a)]. This means that the activation and inactivation functions overlap in the manner that a considerable fraction of the channels are open at steady state membrane voltage. The “window current” actually means that a large part of the dark resting conductance of the photoreceptor is caused by the *shaker*, and, consequently, it is one major determinant of the dark resting potential.

With only ± 5 -mV voltage shifts of *shaker* steady state activation ($act\ g_{inf}$) and inactivation ($inact\ g_{inf}$) it is possible to produce remarkably large or small window current areas. As a sensitivity analysis, these variations were tested with similar simulations as in Fig. 6(a) [Fig. 9(b)]. In these g_{LIC} had to be altered from the normal 0.0529 mS/cm² (in -60 mV) to 0.1120 mS/cm² with the larger and to 0.0081 mS/cm² with the smaller window current area to maintain the -60 mV without stimulus. Results show that with the small window current area the amplification (see later) caused by the *shaker* inactivation is increased and with the larger it is decreased but the amplification effect does not totally vanish.

In addition, a sensitivity analysis was run to consider the situation, when the window current is altered on much wider scale by shifting the inactivation $+10$ mV and shifting the activation from -15 to $+10$ mV, [Fig. 9(c)]. In this analysis any other parameters, including g_{LIC} , were not altered. Results show that with very wide window current area the amplification effect disappears. This is caused by the large *shaker* conductance in wide voltage range and the absence of effective inactivation.

In addition to the resting potential regulation in the *Drosophila* photoreceptors, the *shaker* conductance is able to amplify the responses, as is evident from the current clamp simulations in Fig. 5(a). Here the rapid inactivation

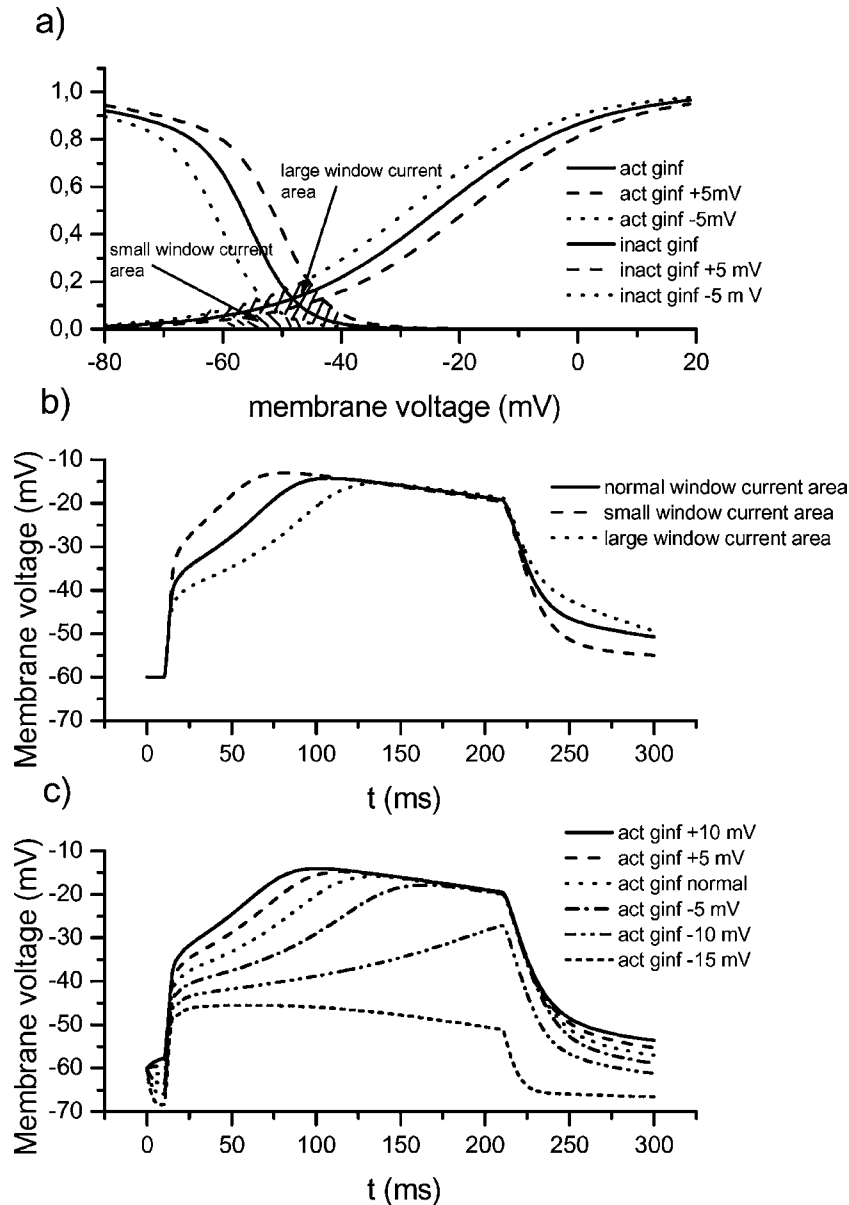


FIGURE 9. (a) *shaker* window current area and variations that cause larger or smaller areas, (b) Effects of window current area variations on the experiment in Fig. 6(a) with *shaker* conductance only, (c) effects of larger area variations.

of the *shaker* conductance increases the depolarizations caused by current injection. The amplification arises from the rapid inactivation following activation of the conductance. In addition, the kinetics of the *shaker* are such that the inactivation causes the conductance to be smaller during long-lasting depolarization than in the resting potential. The same effect is seen in the light response simulations in Fig. 6(a) and Fig. 6(b). There we see the contribution of single conductance types to the response separately. The normal dark adapted membrane with the *shaker* alone produces bigger voltage responses than the passive membrane in the nonmodulated case [Fig. 6(a)]. In other words, the *shaker* inactivation produces signal amplification, because

the balance between the hyperpolarizing (potassium) conductance and the depolarizing (light gated) conductance is shifted in favor of the depolarization. This amplification is similar as in the case of dendrites of vertebrate neurons.⁹ In short flash responses [Fig. 7(a)] the *shaker* does not amplify the peak responses, but prolongs the repolarization. In the terms of signal processing, the longer repolarization would mean longer integration time under these conditions.

When the sole voltage activated conductance is the delayed rectifier [Fig. 6(b); also in Fig. 5(c), where both conductances act qualitatively like delayed rectifiers], a voltage notch is seen at the beginning of the response. This is caused by a slow activation of the delayed rectifier, after which

the membrane voltage tends to go toward the potassium equilibrium potential. The response of the membrane with both conductances is a combination of the responses of membrane with individual conductances [see Fig. 5(d) and Fig. 6]

The concept of signal amplification by an inactivating K^+ conductance may be confusing, because it is based on the ability of the channels to close on depolarization, thereby increasing the membrane resistivity. This then leads to bigger voltage signals if the stimulus, i.e. light activated current remains equal. One obvious proposal would be that for the cell to obtain larger and better amplification it could just have less channels to increase the cell's resistance. But this is not an equivalent situation. The conductance created by voltage activated channels is both voltage- and time-dependent, meaning that it does not function equally in all situations. The behavior of an inactivating conductance, like the *shaker*, is even more complicated. In our opinion we should consider finding the answer to the problem "why channels at all?" from this complicated voltage- and time-dependence. What the *shaker* conductance is obviously doing is amplification of the low or intermediate frequency signals under dim light conditions. The reason, why this particular band of signals has to be amplified, may be found from the behavior of the flies. It might be that the signal-to-noise ratio is so poor in cells with relatively large single photon responses, like in *Drosophila* (when compared to e.g. Calliphora R1–R6 photoreceptors), that to see reasonably well in dim light this kind of booster is needed. In brighter light (more depolarized membrane) the *shaker* is rendered very nearly nonfunctional by the inactivation [Fig. 6(b)]. Following the reasoning of the high metabolic cost of leaky membranes,^{31,32} we may suppose that the most efficient way of amplifying a selective bandwidth of signals, if this is required, would be to do this by closing the channels dynamically with depolarization. In light adaptation, when the metabolic burden of high rate of phototransduction is very high, the *shaker* channels could then be closed, the leak thereby decreased, and the energetic cost would become smaller.

Serotonin Modulation

It is reported that the 5-HT effect on photoreceptor potassium currents of Hermissenda and Aplysia is to decrease the membrane conductance.^{1,10,11} 5-HT decreases the potassium currents by a positive shift of the voltage operating ranges of activation¹¹ in the same manner as shown in *Drosophila*.²⁰ Generally, the 5-HT modulation of the voltage dependent currents has been interpreted in terms of a decrease in the g_{max} and in changes in the time constants of activation and inactivation.⁴³ In our work the shift to a more depolarized range of activation and inactivation of both the *shaker* and the delayed rectifier conductances resulted in a reduction of the delayed rectifier current. The

steady state *shaker* current was enhanced at depolarized voltages due to the shift of the window current area. This shift prevents the *shaker* inactivation from acting as an amplifier, and the 5-HT modulated membrane acts like one with delayed rectifier only [Fig. 6(c) and Fig. 6(d)]. With short flashes (Fig. 7) the situation is somewhat different. There the rapid activation of the *shaker* is actually making the response smaller, but the long tail means amplification of slow signals [Fig. 7(a)]. In the modulated case [Fig. 7(b)] the voltage response to light is significantly larger. This is due to the lesser activation of the *shaker*. The repolarization is also faster, due to the removal of the depolarizing effect of the *shaker* inactivation.

CONCLUSION

We have constructed a membrane model for *Drosophila* photoreceptors with Hodgkin-Huxley type^{21–23} equations for *Drosophila shaker* – (KA) and slowly inactivating delayed rectifier – (KS) conductances, based on experimental data. Thus we could investigate (with simulations) the photoreceptor membrane of *Drosophila* and to do simulation experiments that could be very difficult to do with real cells and show some very important results³⁵ and explain how these results occur. Simulations show typical actions of the delayed rectifier, as described earlier.^{32,41,42} The activation and inactivation of the *shaker* may produce voltage signal amplification over that of the equivalent passive membrane. In addition, the *shaker* is crucial in regulating the resting potential of the cells. The effect of serotonin (5-HT) modulation of voltage dependence of the conductances²⁰ causes the photoreceptor membrane to act more like one with the delayed rectifier only, removing the amplification of the slow responses.

REFERENCES

- Acosta-Urquidi, J., and T. Crow. Differential modulation of voltage dependent currents in Hermissenda type B photoreceptors by serotonin. *J. Neurophysiol.* 70:541–548, 1993.
- Anderson, J., and R. C. Hardie. Different photoreceptors within the same retina express unique combinations of potassium channels. *J. Comp. Physiol. A.* 178:513–522, 1996.
- Barnes, S. After transduction-response shaping and control of transmission by ion channels of the photoreceptor inner segment. *Neuroscience* 58:447–459, 1994.
- Benkenstein, C., M. Schmidt, and M. Gewecke. Voltage activated whole-cell K^+ currents in lamina cells of the desert locust *Schistocerca gregaria*. *J. Exp. Biol.* 202:1939–1951, 1999.
- Bringmann, A., B. Biedermann, and A. Reichenbach. Expression of potassium channels during postnatal differentiation of rabbit Muller glial cells. *Eur. J. Neurosci.* 11:2883–2896, 1999.
- Byrne, J. H. Analysis of ionic conductance mechanisms in motor cells mediating inking behavior in *Aplysia californica*. *J. Neurophysiol.* 43:630–650, 1980.
- Connor, J. A. Slow repetitive activity from fast conductance changes in neurons. *Fed. Proc.* 37:2139–2145, 1978.

- ⁸Connor, J. A., and C. F. Stevens. Predictions of repetitive firing behavior from voltage clamp data on an isolated neurone soma. *J. Physiol.* 213:31–53, 1971.
- ⁹Cook, E. P., and D. Johnston. Active dendrites reduce location-dependent variability of synaptic input trains. *J. Neurophysiol.* 78:2116–2128, 1997.
- ¹⁰Critz, S. D., D. A. Baxter, and J. H. Byrne. Modulatory effects of Serotonin, FMRFamide, and Myomodulin on the duration of action potentials, excitability, and membrane currents in tail sensory neurons of *Aplysia*. *J. Neurophysiol.* 66:1912–1926, 1991.
- ¹¹Farley, J., and R. Wu. Serotonin modulation of Hermissenda type B photoreceptor light responses and ionic currents: Implications for mechanisms underlying associative learning. *Brain Res. Bull.* 22:335–351, 1989.
- ¹²Gerster, U. Light-induced changes in membrane potential in honeybee and blowfly photoreceptors: Quantitative analysis and modelling. Thesis, University of Berlin, 1996.
- ¹³Gerster, U., D. G. Stavenga, and W. Backhaus. Na⁺/K⁺-pump activity in photoreceptors of the blowfly *Calliphora*: A model analysis based on membrane potential measurements. *J. Comp. Physiol. A.* 180:113–122, 1997.
- ¹⁴Hardie, R. C. Functional organization of the fly retina. *Prog. Sens. Physiol.* 5:1–79, 1985.
- ¹⁵Hardie, R. C. Voltage-sensitive potassium channels in *Drosophila* photoreceptors. *J. Neurosci.* 11:3079–3095, 1991.
- ¹⁶Hardie, R. C. Phototransduction. The invertebrate enigma. *Nature* 11:113–114, 1993.
- ¹⁷Hardie, R. C., and B. Minke. The *trp* gene is essential for a light-activated Ca²⁺ channel in *Drosophila* photoreceptors. *Neuron* 8:643–651, 1992.
- ¹⁸Hardie, R. C., D. Voss, O. Pongs, and S. B. Laughlin. Novel potassium channels encoded by the Shaker locus in *Drosophila* photoreceptors. *Neuron* 6:477–486, 1991.
- ¹⁹Hardie, R. C., and M. Weckström. Three classes of potassium channels in large monopolar cells of the blowfly *Calliphora vicina*. *J. Comp. Physiol. A.* 167:723–736, 1990.
- ²⁰Hevers, W., and R. C. Hardie. Serotonin modulates the voltage dependence of delayed rectifier and Shaker potassium channels in *Drosophila* photoreceptors. *Neuron* 14:845–856, 1995.
- ²¹Hille, B. *Ionic Channels of Excitable Membrane*. Sunderland, UK: Sinauer Associates, 1992, p. 607.
- ²²Hodgkin, A. L., and A. F. Huxley. A quantitative description of membrane current and its application to conduction and excitation in nerve. *J. Physiol.* 117:500–544, 1952.
- ²³Johnston, D., and S. S.-M. Wu. *Foundations of Cellular Neurophysiology*. Cambridge, MA: MIT Press, 1997, p. 676.
- ²⁴Juusola, M. Linear and nonlinear contrast coding in light adapted blowfly photoreceptors. *J. Comp. Physiol. A* 172:511–521, 1993.
- ²⁵Juusola, M., and R. C. Hardie. Light adaptation in *Drosophila* photoreceptors: I. Response dynamics and signalling efficiency at 25 degrees C. *J. Gen. Physiol.* 117:3–25, 2001.
- ²⁶Juusola, M., and R. C. Hardie. Light adaptation in *Drosophila* photoreceptors: II. Rising temperature increases the bandwidth of reliable signaling. *J. Gen. Physiol.* 117: 27–42, 2001.
- ²⁷Juusola, M., and M. Weckström. Band-pass filtering by voltage dependent membrane in an insect photoreceptor. *Neurosci. Lett.* 154:84–88, 1993.
- ²⁸Kaczmarek, L. K., and I. B. Levitan. *Neuromodulation. The Biochemical Control of Neuronal Excitability*. Oxford: Oxford University Press, 1987, p. 286.
- ²⁹Kawai, F., and E. Miyachi. Odorants suppress voltage-gated currents in retinal horizontal cells in goldfish. *Neurosci. Lett.* 281:151–154, 2000.
- ³⁰Lasater, E. M. Membrane-properties of distal retinal neurons. *Prog. Retin. Res.* 11:215–246, 1991.
- ³¹Laughlin, S. B. “Coding efficiency and design in visual processing.” In: *Facets of Vision*, edited by R. C. Hardie and D. Stavenga. Berlin: Springer, 1989, pp. 213–234.
- ³²Laughlin, S. B., and M. Weckström. Fast and slow photoreceptors—a comparative study of the functional diversity of coding and conductances in the Diptera. *J. Comp. Physiol.* 172:593–609, 1993.
- ³³Laurent, G. Evidence for voltage activated outward currents in the neuropilar membrane of locust nonspiking local interneurons. *J. Neurosci.* 11:1713–1726, 1991.
- ³⁴Mascagni, M. V., and A. S. Sherman. “Numerical methods for neuronal modeling.” In: *Methods in Neuronal Modeling: From Ions to Networks*, 2nd ed., edited by C. Koch and I. Segev. Cambridge, MA: MIT Press, 1998, pp. 569–606.
- ³⁵Niven, J. E., M. Vähäsöyrinki, M. Kauranen, R. C. Hardie, M. Juusola, and M. Weckström. The contribution of *shaker* K⁺ channels to the information capacity of *Drosophila* photoreceptors. *Nature* 421:630–634, 2003.
- ³⁶Postma, M., J. Oberwinkler, and D. Staving. Does Ca²⁺ reach millimolar concentrations after single photon absorption in *Drosophila* photoreceptor microvilli? *Biophys. J.* 77:1811–1823, 1999.
- ³⁷Ranganathan, R., G. L. Harris, C. F. Stevens, and C. S. Zuker. A *Drosophila* mutant defective in extracellular calcium-dependent photoreceptor deactivation and rapid desensitization. *Nature* 354:230–232, 1991.
- ³⁸Rush, M. E., and J. Rinzel. The potassium A-current, low firing rates and rebound excitation in Hodgkin-Huxley models. *Bull. Math. Biol.* 57:899–929, 1995.
- ³⁹Shimatani, Y., and Y. Katagiri. Light removes inactivation of the a-type potassium channels in scallop hyperpolarizing photoreceptors. *J. Neurosci.* 15:6489–6497, 1995.
- ⁴⁰Weckström, M. Voltage dependent outward currents in adult and nymphal locust photoreceptors. *J. Comp. Physiol. A* 174:795–801, 1994.
- ⁴¹Weckström, M., R. C. Hardie, and S. B. Laughlin. Voltage-activated potassium channels in blowfly photoreceptors and their role in light adaptation. *J. Physiol.* 440:635–657, 1991.
- ⁴²Weckström, M., and S. B. Laughlin. Visual ecology and voltage gated ion channels in insect photoreceptors. *Trends Neurosci.* 18:17–21, 1995.
- ⁴³White, J. A., D. A. Baxter, and J. H. Byrne. Analysis of the modulation by serotonin of a voltage dependent potassium current in sensory neurons of *Aplysia*. *Biophys. J.* 66:710–718, 1994.
- ⁴⁴Yazulla, S., and K. M. Studholme. Differential distribution of Shaker-like and Shab-like K⁺-channel subunits in goldfish retina and retinal bipolar cells. *J. Comp. Neurol.* 396:131–140, 1998.
- ⁴⁵Zagotta, W. N., and R. W. Aldrich. Alterations in activation gating of single Shaker A-type potassium channels by the Sh⁵ mutation. *J. Neurosci.* 10(6):1799–1810, 1990.